From Humorous Post to Detailed Quantum-Chemical Study: Isocyanate Synthesis Revisited

Oleg B. Beletsan[1], Igor Gordiy[2], Sergey S. Lunkov[1,3], Mikhail A. Kalinin[1], Larisa E. Alkhimova[4,5], Egor A. Nosach[6], Egor A. Ilin[1,3], Alexandr V. Bespalov[7], Olgert L. Dallakyan[8], Aleksandr A. Chamkin[9], Ilya V. Prolomov[10,3], Radion A. Zaripov[11], Andrey A. Pershin[12,13], Bogdan O. Protsenko[14], Yury V. Rusalev[14], Ruslan A. Oganov[15], Diana K. Kovaleva[15], Vladimir A. Mironov[16], Victor V. Dotsenko[7,17], Alexandr M. Genaev*[18], Dmitry I. Sharapa†[19], and Denis S. Tikhonov‡[19]

[1]Department of Chemistry, Lomonosov Moscow State University, 119991 Moscow, Russia
[2]ChemU Corporation Ltd., 3106 Limassol, 17 17 Gr. Xenopoulou St., Cyprus
[3]N. D. Zelinsky Institute of Organic Chemistry, 119991 Moscow, Leninsky prosp. 47, Russia
[4]Center for Nature-Inspired Engineering, University of Tyumen, 625003 Tyumen, Russia
[5]Institute of Chemistry, University of Tyumen, 625003 Tyumen, Russia
[6]Department of Fundamental Physical and Chemical Engineering, Lomonosov Moscow State University, 119234 Moscow, Russia
[7]Department of Chemistry and High Technologies, Kuban State University, 149 Stavropolskaya st., 350040 Krasnodar, Russia
[8]Computational Material Science Laboratory, Department of Physics, Yerevan State University, 0025 Yerevan, Armenia
[9]A.N.Nesmeyanov Institute of Organoelement Compounds of Russian Academy of Sciences, 119334 Moscow, Russia
[10]D. Mendeleev University of Chemical Technology of Russia, 125047 Moscow, Russia
[11]Skolkovo Institute of Science and Technology, 121205 Moscow, Russia
[12]Samara Branch of Lebedev Physical Institute, 443011 Samara, Russia
[13]Department of Physics, Samara University, 443086 Samara, Russia
[14]The Smart Materials Research Institute, Southern Federal University, 344090 Rostov-on-Don, Russia
[15]Department of Biochemistry, Lomonosov Moscow State University, 119991 Moscow, Russia
[16]A. M. Butlerov Chemistry Institute, Kazan Federal University, 420008 Kazan, Russia
[17]Faculty of Chemistry and Pharmacy, North-Caucasus Federal University, 355017 Stavropol, Russia
[18]N.N. Vorozhtsov Institute of Organic Chemistry, 630090 Novosibirsk, Russia.
[19]Independent researcher

February 9, 2024

*Corresponding Author: genaev@nioch.nsc.ru
†Corresponding Author: gess87@mail.ru
‡Corresponding Author: madschumacher@yandex.ru

Abstract

Isocyanates play an essential role in modern manufacturing processes, especially in polyurethane production. There are numerous synthesis strategies for isocyanates both in industrial and laboratory conditions, which do not prevent searching for alternative highly efficient synthetic protocols. Here, we report a detailed theoretical investigation of the mechanism of sulfur dioxide-catalyzed rearrangement of the phenylnitrile oxide into phenyl isocyanate, which was first reported in 1977. The DLPNO-CCSD(T) method and up-to-date DFT protocols were used to perform a highly accurate quantum-chemical study of the rearrangement mechanism. An overview of various organic and inorganic catalysts has revealed other potential catalysts, such as sulfur trioxide and selenium dioxide. Furthermore, the present study elucidated how substituents in phenylnitrile oxide influence reaction kinetics. This study was performed by a self-organized collaboration of scientists initiated by a humorous post on the VK social network.

1 Introduction

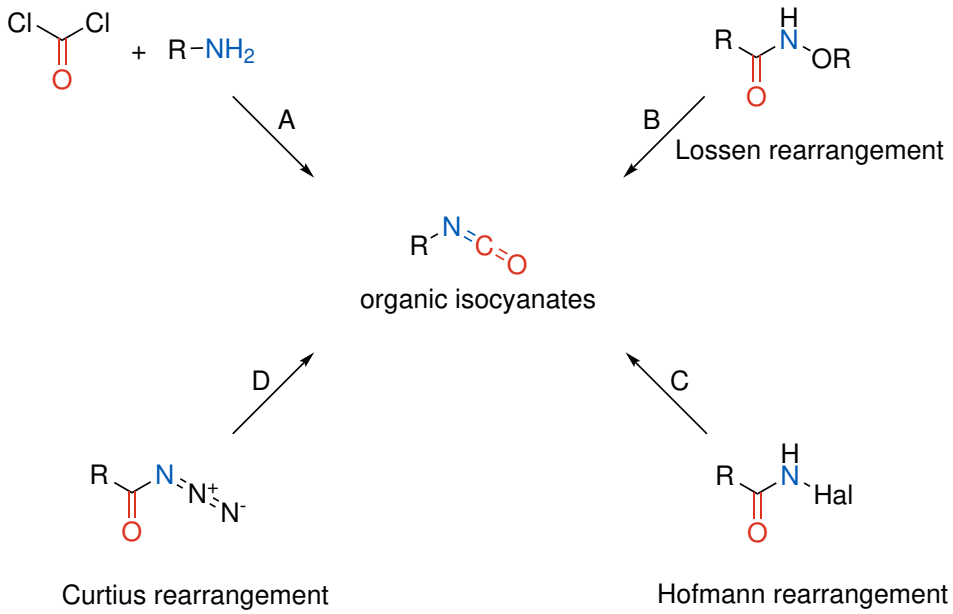

Figure 1: A general scheme of the existing synthetic approaches to isocyanates.

Isocyanates are important and versatile reagents for both fine and large-scale organic synthesis.[1–4] The main use of isocyanates is the production of widely used polyurethanes (PU) – indispensable component in the manufacturing process of protective coatings, adhesives, dyes, sealants, various wear-resistant materials, biomaterials, etc.[5–8] In addition, methyl isocyanate is an important intermediate in the synthesis of carbamate pesticides.[9] The large-scale manufacture of isocyanate is usually based on the reaction of amines with toxic phosgene (Figure 1, reaction A). On a laboratory scale, isocyanates are usually prepared by one of the rearrangement reactions – e.g., Lossen rearrangement (Figure 1, reaction B),[10] Hofmann rearrangement (Figure 1, reaction C),[11] and Curtius rearrangement (Figure 1, reaction D).[12, 13] At the same time, alternative approaches toward isocyanates have also been described in the literature. One such reaction is the thermal or catalyzed rearrangement of nitrile oxides.[14]

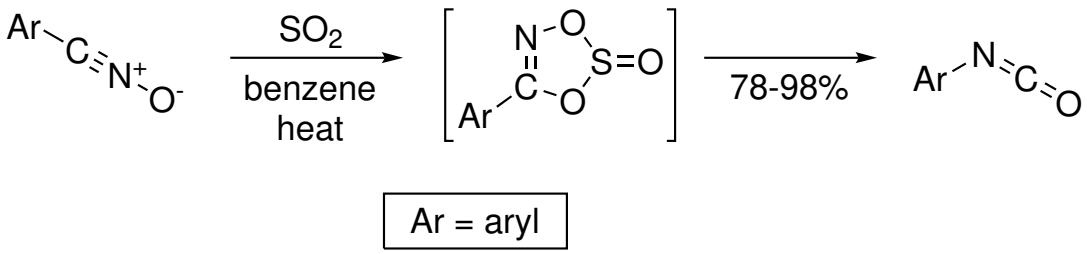

Figure 2: A proposed mechanism of isomerization reaction from nitrile oxides to isocyanate catalyzed by SO_2 from Ref. [14] found in the initializing post in the VK social network.[15]

Possible pathways of rearrangement between isomeric nitrile oxides (R−C≡N$^+$−O$^-$), cyanates (R−O−C≡N), and isocyanates (R−N=C=O) have captivated the attention of chemists for over a century.[16] Since the development of computational chemistry, numerous studies have aimed to explain the nitrile-oxide-to-isocyanate isomerization;

however, usually, the objects were "spherical ~~cows~~ molecules in a vacuum."[17] Thus, chemically unreliable barriers exceeding 50 and sometimes even 80 kcal/mol were obtained.[18–21] In 1977, fascinatingly illogical isomerization from nitrile oxides to isocyanate under relatively mild conditions was demonstrated, but remained almost unnoticed (see Figure 2).[14] Authors speculated that the reaction proceeds through the 1,3-dipolar cycloaddition (Huisgen reaction), and thus isomerization is an oxygen exchange, with SO_2 playing an atypical role of a catalyst. This assumption also bridges the suggested mechanism with a reaction between nitrile oxides and sulfinylamines that results in carbodiimides.[22, 23] However, such a chemical transformation caused some confusion when one of our research team members came across a post on the VK social network.[15] Thus, an idea to create a crowd-effort project to study this rearrangement pathway came out. The result of this was the creation of self-organized collaboration, initiated with the corresponding post in the VK social network.[24]

In the current study, we present a detailed state-of-the-art *in silico* mechanistic investigation of the reaction mechanism of SO_2-catalyzed conversion of phenylnitrile oxide into phenyl isocyanate. Based on the established reaction mechanism, we conduct a theoretical screening of other potential inorganic and organic catalysts. In the final part of the study, we also provide a screening of other possible substrates and their influence on the reaction's kinetics.

2 Results and discussion

2.1 SO_2-catalyzed conversion of phenylnitrile oxide into phenyl isocyanate

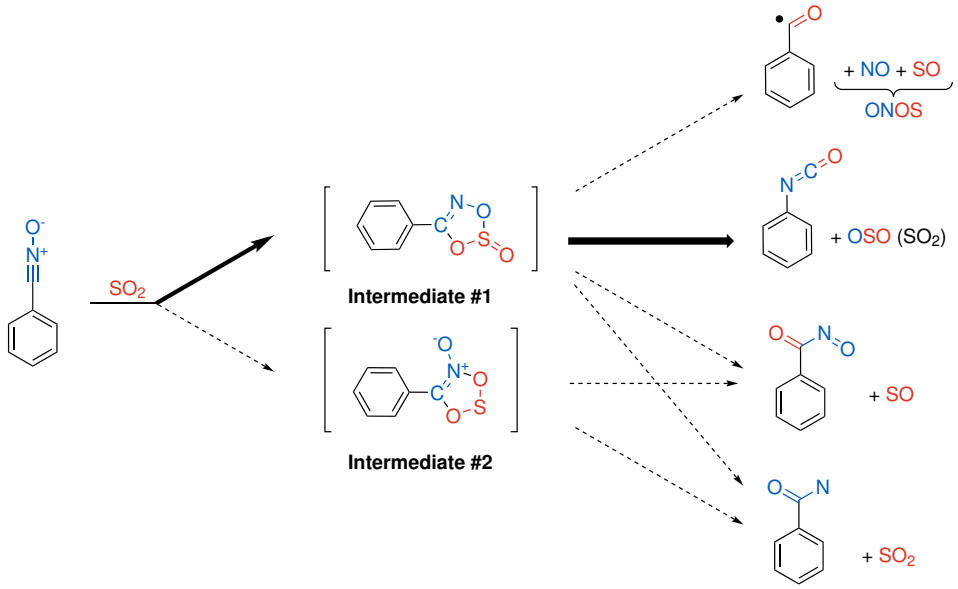

Figure 3: The results of the initial screening of the probable reaction pathways for phenylnitrile oxide and SO_2 system at the B3LYP-D3(BJ)/6-31G level of theory. The bold solid arrows indicate the only feasible reaction mechanism. The colors of the atoms illustrate whether they initially belong to the reactant (blue) or catalyst (red).

To explore the chemical space of the original conversion reaction of nitrile oxide into isocyanate in greater detail, we first screened the possible pathways at B3LYP-D3(BJ)/6-31G level of theory in the gas phase. The results of this screening are outlined in Figure 3. We explored two main pathways, proceeding through two possible intermediates, denoted as Intermediate #1 and #2. Intermediate #1 resembles the initially assumed mechanism (see initial post), in which the whole nitrile oxide ($C{\equiv}N^{+}{-}O^{-}$) group of the reactant and a single S=O bond of the SO_2 participate in [3+2]-cycloaddition to form a five-membered ring. In the Intermediate #2, a similar process occurs with the whole SO_2 and $C{\equiv}N^{+}$ part of the $C{\equiv}N^{+}{-}O^{-}$-group.

The pathways for both intermediates were explored by manual chemical intuition-guided transition state (TS) search. In addition, metadynamics (MTD) simulations of the Intermediate #1 were performed with three different collective variables. The full set of results can be found in the electronic supplementary information (ESI). Various possible chemical outcomes were identified, as shown in Figure 3. However, only phenyl isocyanate (PhNCO) was an exothermic reaction product with a low enough barrier of 35.9 kcal/mol separating the Intermediate #1 from the products. In the case of the alternative pathway through Intermediate #2, the rate-limiting step had a barrier of 46.4 kcal/mol. Therefore, we can ignore other found products and mechanisms as highly improbable and focus on the reaction of SO_2-catalyzed conversion of phenylnitrile oxide into phenyl isocyanate, proceeding through the Intermediate #1.

We have calculated the intermediate states and TS of the most probable pathway in Figure 3 using various methods and approaches (details are given in ESI). To confirm, that the mechanism indeed proceeds only through two TS, we have performed the intristic reaction coordinate (IRC) scans for both of these TS. The results at the r^2SCAN-3c level

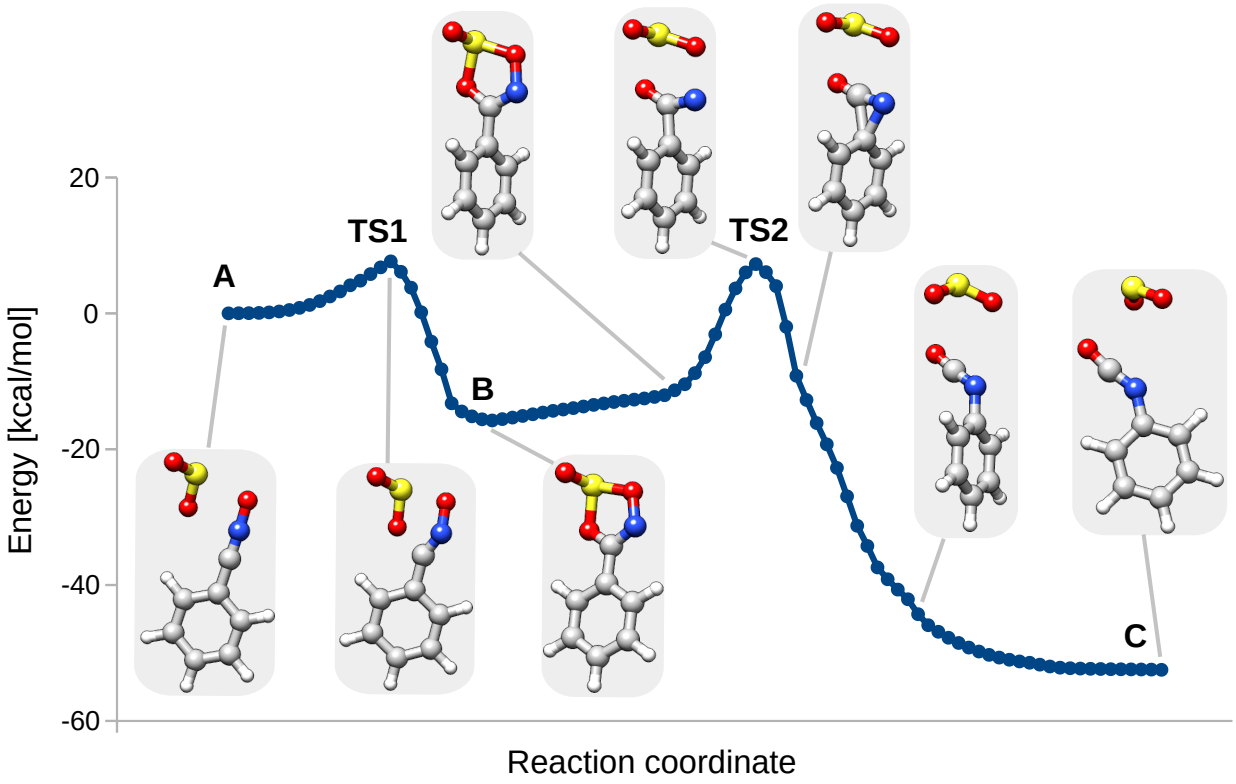

Figure 4: Concatenated IRC plots for the reaction of phenylnitrile oxide conversion to into phenyl isocyanate catalyzed with SO_2 calculated by r2SCAN-3c/CPCM(toluene) method (ORCA program).

of theory in toluene is shown in Figure 4, and more IRC scans, including the animations, are given in the ESI. As we can see, the reaction indeed proceeds upon a formation of the intermediate cyclic adduct, which then converts into the isocyanate in a single step. To ensure that we are not missing an intermediate structure in this complex motion, we performed an additional relaxed internal rotation scan for the internal rotation of two rings was made at the ωB97x-D3(BJ)/def2-TZVPPD level of theory in both gas phase and benzene. No stable conformer of the intermediate B was found (results are shown in ESI).

The mechanism of the phenylnitrile oxide conversion to into phenyl isocyanate catalyzed with SO_2 presented in Figure 4 can be described with the following kinetic scheme:

$$\text{Reagents} \leftrightharpoons \text{A} \leftrightharpoons \text{B} \rightarrow \text{C} \leftrightharpoons \text{Products} \ . \tag{1}$$

First, the reactant (PhCNO) forms a pre-intermediate A with the catalyst (SO_2). Then, it converts into the intermediate B by a [3+2]-cycloaddition through the transition state TS1. Then, the intermediate B converts into products through the TS2. In this case, the newly formed five-membered ring rotates by 90° with respect to the phenyl ring, and the nitrogen moves towards the phenyl group. Then, the post-intermediate C is produced, which is a complex of the reaction product (PhNCO) with the catalyst, and in the end, they dissociate into separate species.

The resulting mechanism was recomputed by various high-level pure DFT and composite methods (computational details are thoroughly described in ESI) in the gas and liquid (benzene, toluene solvents) phases emulated with the CPCM and COSMO continuum models. Here, we will base our discussion on the reaction pathways computed in benzene with a composite method of DLPNO-CCSD(T)/CBS//DFT, where the DFT method used is either r^2SCAN-3c or ωB97X-D3(BJ)/def2-TZVPP, as shown in Figure 5. The reference reaction pathway was computed with a ZORA DLPNO-CCSD(T1) protocol that involved both CBS and infinite PNO space extrapolation.[26] These calculations were based on r^2SCAN-3c geometries. We compared these results with the DLPNO(NormalPNO)-CCSD(T)/CBS//DFT and pure DFT results. The standard deviations (SD) for the reaction pathway were below 1 kcal/mol for DLPNO(NormalPNO)-CCSD(T)/CBS results, while pure DFT calculations differed more significantly, exceeding the chemical accuracy by 2-4 kcal/mol. Therefore, further discussions on the other reaction pathways will be based on the DLPNO-CCSD(T)/CBS//r^2SCAN-3c results, as they match the benchmark calculations with nearly chemical accuracy.

To compare the reaction pathways with each other, it is advantageous to represent them with a single number. For that, we propose a simplified chemical model. We can assume that pre-intermediate A and post-intermediate C are in equilibrium with reagents and products, respectively. A and B are connected through TS1, and the conversion from B to C is irreversible due to the largest barrier of 72 kcal/mol 5. By applying a steady state approximation[27] for the catalyst (SO_2) and Intermediate #1 (B), details are given in ESI, we can describe this scheme with a single

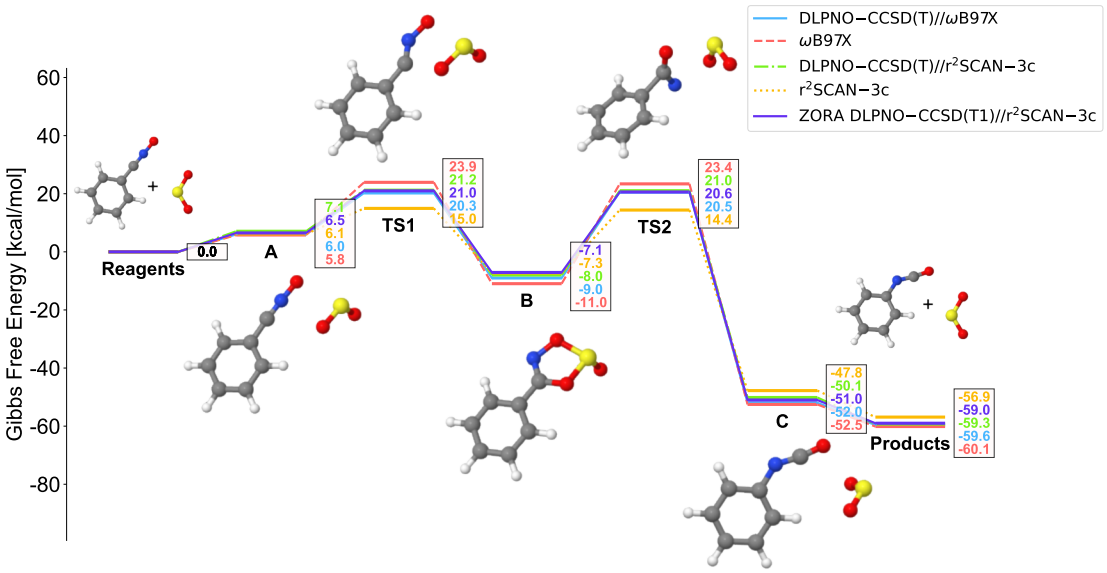

Figure 5: Computed reaction pathways of the SO_2-catalyzed conversion of phenylnitrile oxide into phenyl isocyanate at the various levels of theory in the benzene simulated with CPCM continuum solvation model. The "DLPNO" denotes DLPNO(NormalPNO)-CCSD(T)/CBS(3/4) single point energies. The "ωB97X" denotes ωB97X-D3(BJ)/def2-TZVPP level of theory. Here, the standard Jmol[25] atom coloring scheme is used. White atoms are hydrogens, gray are carbons, blue are nitrogens, red are oxygens, and yellow are sulfur.

effective reaction barrier

$$\Delta G^{\ddagger}_{\text{eff}} = \Delta G^{\ddagger}_{\text{AB}} + \Delta G_{\text{RA}} - \Delta G_{\text{PC}} + k_{\text{B}}T \ln\left(1 + \exp\left(\frac{\Delta G^{\ddagger}_{\text{BC}} - \Delta G^{\ddagger}_{\text{BA}}}{k_{\text{B}}T}\right)\right) , \tag{2}$$

where $k_{\text{B}} = 1.38 \times 10^{-23}$ J/K is the Boltzmann constant, T is the absolute temperature, $\Delta G^{\ddagger}_{XY}$ is the Gibbs free energy barrier for a transition from state X to state Y at a given temperature, ΔG_{PC} is the Gibbs free energy of the reaction step Products → C, and ΔG_{RA} is the Gibbs free energy of the reaction step Reagents → A. This barrier provides an estimate of the rate of an effective reaction Reagents ⟶ Products with a rate constant given by the Eyring–Polanyi equation:[28, 29]

$$k_{\text{eff}} = \frac{k_{\text{B}}T}{h} \exp\left(-\frac{\Delta G^{\ddagger}_{\text{eff}}}{k_{\text{B}}T}\right) , \tag{3}$$

where $h = 6.63 \times 10^{-34}$ J·s is the Planck constant. This effective energy barrier $\Delta G^{\ddagger}_{\text{eff}}$ from Equation 2 at $T = 298$ K will be later used for comparison of the modifications of the original reaction.

2.2 Survey of other possible solvents

First, we provided a survey of how the solvent influences the reaction (Figures 2) kinetics going through the two-TS mechanism (Figures 4 and 5). For this, we took the gas-phase calculation of the reaction at the DLPNO-CCSD(T)/CBS//r^{2}SCAN-3c level of theory and applied the recently developed Solv model,[30] applied in SPT-V scheme. We have selected 28 of the most common laboratory solvents, ranging from nonpolar (hexane, carbon disulfide) to the most polar (water). The studied solvents span a substantial polarity range, allowing us to explore the polarity influence on the effective reaction barrier height. It was decided to use two well-established polarity descriptors: the relative dielectric constant and Reichardt's polarity parameters. The latter one was introduced by Reichardt *et al* in 1963 and since then has been extensively used for studies involving solvent polarity. [31–35] The full list of the studied solvents, as well as the corresponding dielectric constant and Reichardt's parameter values, can be found in ESI. The correlations of the effective barrier heights (Equation 2) with solvents' dielectric constants ε and Reichardt's $E_T(30)$ parameters are shown in the Figure 6. The polarity of the solvent increases with increasing ε and $E_T(30)$, and as we can see from the results, the increase of the polarity of the solvent decreases the effective reaction barrier, making the reaction faster. It is worth noting that the effect of solvent polarity on the effective reaction barrier height is not dramatic since the maximum difference observed for water (the most polar solvent studied) is still less than 1 kcal/mol. It is consistent with the previously reported observations that the pericyclic reactions are not sensitive to solvent polarity due to the absence of significant degree of charge separation in a course of the reaction.[36]

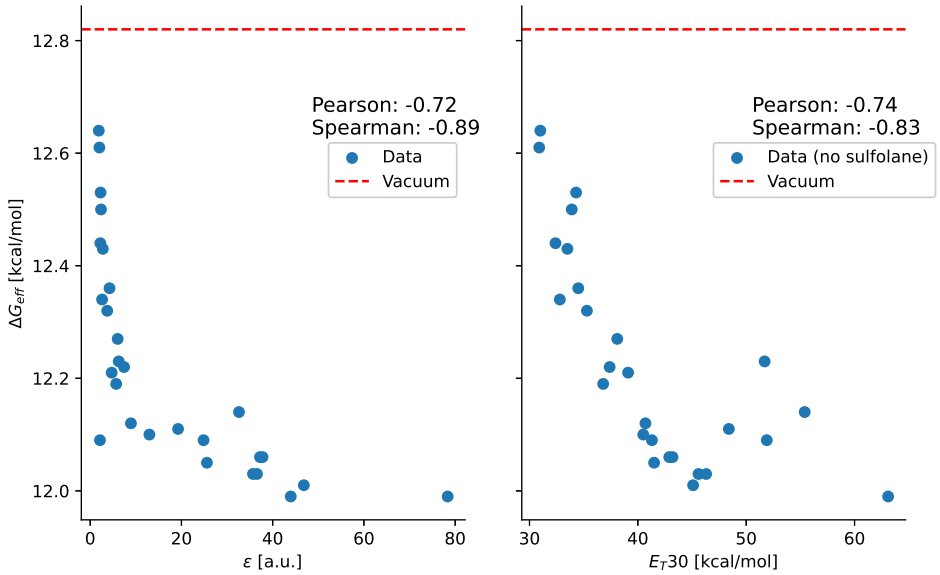

Figure 6: Survey of change in effective reaction free energy barrier (Equation 2) for 42 solvents of various polarity. The gas-phase energies were computed at the DLPNO-CCSD(T)/CBS//r^{2}SCAN-3c, while the free-energy correction for solvation was computed within Solv model[30] applied in the SPT-V scheme. Sulfolane has been excluded from the correlation plot with $E_T(30)$ parameters since, to the best of our knowledge, no value for it has been reported in the literature so far.

2.3 Survey of other possible catalysts

2.3.1 Inorganic catalysts

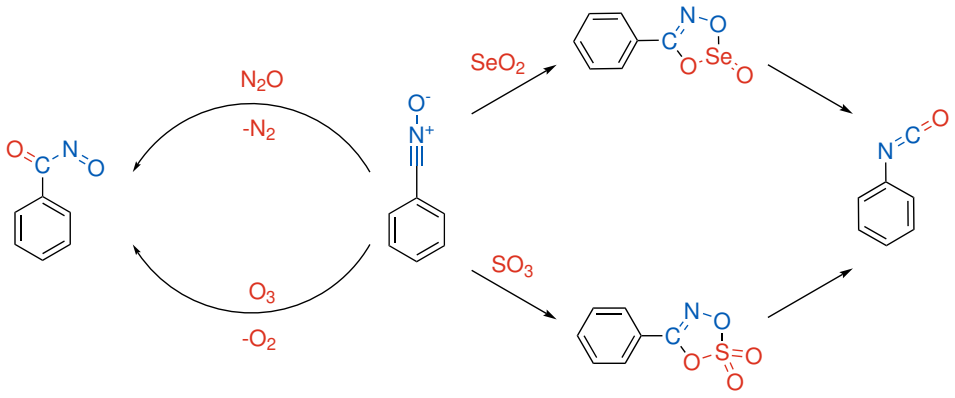

Figure 7: Summary of reaction pathways identified in the inorganic catalysts survey for the phenylnitrile oxide into isocyanate conversion. The effective barrier height (Equation 2) in benzene at DLPNO-CCSD(T)/CBS//r^{2}SCAN-3c level of theory were the following. The original reaction's (Figure 3) effective barrier is 12 kcal/mol, for SeO_2 as a catalyst, it is 3 kcal/mol, for SO_3 as a catalyst, the reaction in the same treatment is barrier-less. The colors of the atoms illustrate whether they initially belong to the reactant (blue) or catalyst (red).

To investigate other possible catalysts, we considered a set of small three-atomic molecules: ozone (O_3), selenium dioxide (SeO_2), and nitrous oxide (N_2O). O_3 and SeO_2 were chosen as direct analogs of the SO_2.[37–39] SeO_2 is also a ubiquitously used organic catalyst.[40–42] In addition, sulfur trioxide (SO_3) was also tested, as it was shown to produce a similar intermediate in a tetrahydrofuran (THF) medium.[43]

The found reactive pathways for the chosen inorganic molecules are shown in Figure 7. For ozone and nitrous oxide, we did not find any path leading to the desired phenyl isocyanate, as they tend to oxidize the molecule into N-oxobenzamide. SeO_2 and SO_3 follow the same pathway as SO_2 yielding the desired compound. The effective barrier height (Equation 2) in benzene with SO_2 as a catalyst is 12 kcal/mol, whereas with SeO_2 it is only 3 kcal/mol, i.e., it should be a more active catalyst than the original. SO_3 in THF gives an effectively barrier-less reaction, which probably indicates the nonphysical nature of assumptions made in the derivation of Equation 2 for this particular pathway. However, the barrier from the intermediate towards the products is lower by 2 kcal/mol, which indicates SO_3 also being a superior catalyst compared to the SO_2.

2.3.2 Organic catalysts

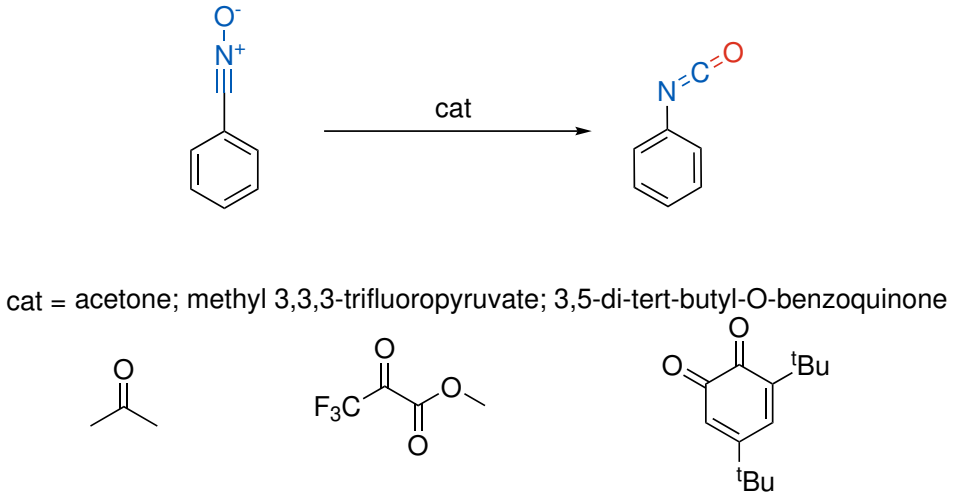

Figure 8: Summary of the reaction pathways identified in the organic ketones survey for the nitrile oxide into isocyanate conversion. The colors of the atoms illustrate whether they initially belong to the reactant (blue) or catalyst (red).

As an alternative organic catalyst, we first briefly investigated the possibility of replacing the S=O moiety with C=O in the [3+2]-cycloaddition leading to the intermediate formation. The initial screening was done using the r^{2}SCAN-3c method in the gas phase. For this, we tested acetone, methyl 3,3,3-trifluoropyruvate, and 3,5-di-*tert*-butyl-*o*-benzoquinone (Figure 8). All these compounds can provide a similar reaction pathway as the SO_2 through the 1,3-dipolar cycloaddition reaction.[44–46] The computed effective reaction barrier (Equation 2) in the gas phase for the SO_2 at the r^{2}SCAN-3c level of theory is 9 kcal/mol, whereas for acetone it is 17 kcal/mol, for methyl 3,3,3-trifluoropyruvate it is 11 kcal/mol, and for 3,5-di-tert-butyl-O-benzoquinone it is 10 kcal/mol. Thus, all investigated alternative organic molecules are predicted to be significantly less effective catalysts for the reaction of interest.

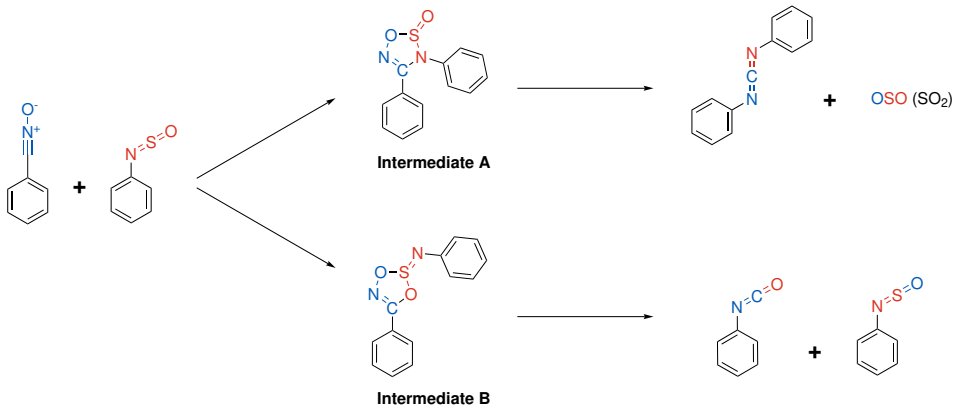

Figure 9: Summary of the reaction pathways for the phenylnitrile oxide reaction with N-sulfinylaniline. The two products are diphenyl carbodiimide (from Intermediate A) and phenyl isocyanate (from Intermediate B). The effective barrier height (Equation 2) in THF at DLPNO-CCSD(T)/CBS//r^{2}SCAN-3c level of theory were the following: for a pathway through Intermediate A is 19 kcal/mol, while for a pathway through Intermediate A is 23 kcal/mol. The colors of the atoms illustrate whether they initially belong to the reactant (blue) or catalyst (red).

As an example of an organic catalyst participating in [3+2]-cycloaddition with nitrile oxide through the S=O bond, we chose N-sulfinylaniline (Ph−N=S=O). However, unlike SO_2, which is symmetric in the [3+2]-cycloaddition reaction, PhNSO is asymmetric, leading to the two possible intermediates that are labeled A and B as shown in Figure 9, where PhNSO is a reactant in pathway A and a catalyst in pathway B. The product arising from the intermediate A is diphenyl carbodiimide (Ph−N=C=N−Ph), while the intermediate B leads to the catalytic conversion of phenylnitrile oxide into phenyl isocyanate. The effective reaction barrier in THF for the pathway A is calculated to be 19 kcal/mol. In contrast, the effective reaction barrier for the pathway B is remarkably higher (23 kcal/mol). Therefore, the simple estimation of the selectivity from the rate constants is given by Eyring–Polanyi equation (3). The ratio of these constants is 860:1, with reaction pathway A being the preferred one.

More detailed kinetic modeling of the parallel reactions (A) and (B) involving reagents PhCNO and PhNSO predicts reaction (A) to be the main pathway, which is in line with the previously obtained experimental data.[47, 48] Furthermore, non-negligible amounts (7% at 298 K, 12% at 383 K) of the corresponding product are predicted to

form via the pathway (B). Thus, it is hypothesized that the PhNSO compound formerly obtained in 14-18% yield in benzene is a product of the parallel reaction (B) and not the unreacted reagent.[48] It should be noted that upon changing the solvent from benzene to diethyl ether, the reagents are not purified from the final reaction mixture.[47] These observations are consistent with the results of *in silico* investigations: barrier heights of the first reaction steps (determining the ratio of the final product) in the pathways (A) and (B) are predicted to differ by 1.5 and 2.2 kcal/mol for reactions in benzene and in THF, respectively. The difference between the barrier heights determines the higher selectivity for reaction in THF compared to that in benzene. The explicit kinetic modeling was based on the rate constants calculated with the Eyring-Polanyi equation, which uses the Gibbs free energies of the transition states. These values were obtained with the state-of-the-art *ab-initio* method DLPNO-CCSD(T)/CBS//ωB97X-D3(BJ)/def2-TZVP in CPCM(THF).

2.4 Survey of substrates

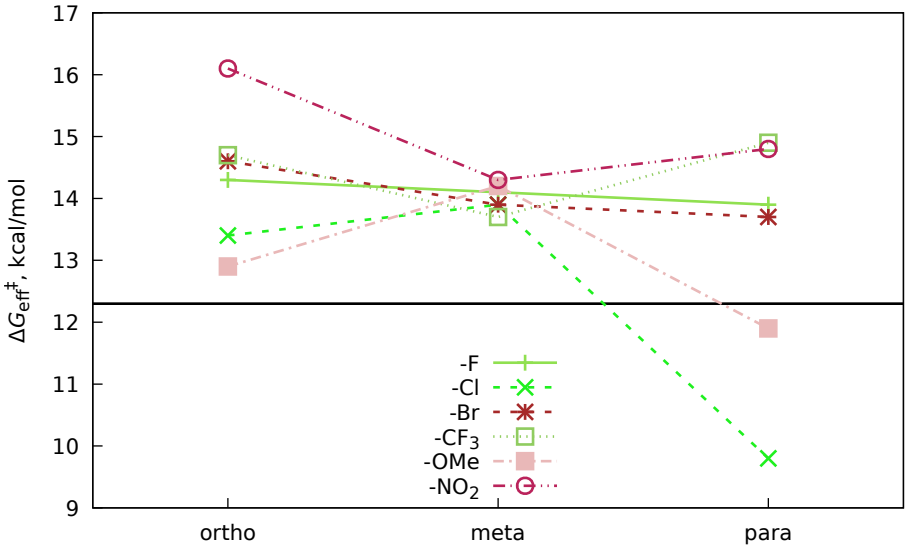

Figure 10: Effective reaction barriers (Equation 2) for the substituted phenylnitrile oxides. The x-axis denotes the substitution position. A solid horizontal line is an effective barrier for the unsubstituted species (12 kcal/mol).

The last effect that was studied is the substitution of the phenyl ring with various substituents, in particular, fluorine (−F), chlorine (−Cl), bromine (−Br), methoxy (−OMe), trifluoromethyl (−CF_3), and nitro (−NO_2) groups. The resulting changes in the effective reaction barrier are summarized in Figure 10. From there, we observe (Figure 10) that all the electron-withdrawing groups, in general, slow down the conversion reaction, except for the *p*-Cl substituted PhCNO, where the effective barrier decreases, and the *o*- and *p*-OMe substituted cases, where the effective barrier stays almost the same (within 0.5 kcal/mol in difference). The *m*-substituted derivatives show very similar activation energies, whether in the cases of the *o*- and *p*-substituted PhCNO, we see a larger spread in reachable energies.

To rationalize the observed trend of effective activation energies, we have tried to correlate these changes with descriptors, characterizing the coupling between the phenyl ring (Ph) and the benzonitrile oxide group −CNO. The descriptors used were the bond order of the Ph−CNO formally single bond and the net atomic charge of the phenyl group. Mayer bond orders were tested, whereas for the atomic charges, we used Mulliken, Löwdin, and Hirshfeld partitions. The results can be seen in Figure 11. Detailed information is available in the Excel file in the ESI.

The highest absolute values of Pearson correlation coefficient (PCC) were observed in the case of Hirshfeld charges for a benzene ring with a substituent and it generally demonstrates a negative correlation. This trend is valid for TS1 and TS2 as well. Interestingly, PCC in the gas phase for reagent and TS2 is identical and equals –0.74. The same tendency is observed in the condensed phase, yielding PCCs of comparable magnitude for reagent and TS2 (–0.61 and –0.64, respectively). Furthermore, PCCs for TS1 are –0.45 and –0.47 in the gas phase and benzene accordingly. This suggests that the reagent and TS2 are more affected by the nature of the substituents, although the PCC is still low to establish a clear relationship with the effective reaction barrier. We collected Mayer bond orders and bond lengths (Å) and determined the PCC with the corresponding effective Gibbs free energy values. The correlation is weak for all cases, especially for the bond order with $\Delta G_{\text{eff}}^{\ddagger}$, for which PCC correlation coefficient is close to zero. The smallest bond orders of R−C_6H_4−CNO bond were detected for *m*-substituted reagents and the shortest bond lengths – for *o*-substituted reagents. Moreover, the bond order growth was observed in *m*-F < *m*-Br < *m*-Cl < *m*-MeO < m-CF_3 < *m*-H < *m*-NO_2 row, and almost the same row was obtained for bond lengths: *o*-NO_2 < *o*-F < *o*-Cl < *o*-Br < *o*-MeO. No other dependencies have been identified. The row of growing bond order is difficult to interpret, whereas the row of growing bond length does not contradict the chemical intuition and corresponds well with $\Delta G_{\text{eff}}^{\ddagger}$ values. Thus, an increase of electron-acceptor properties of the substituent in the *o*-position slows down the chemical reaction with

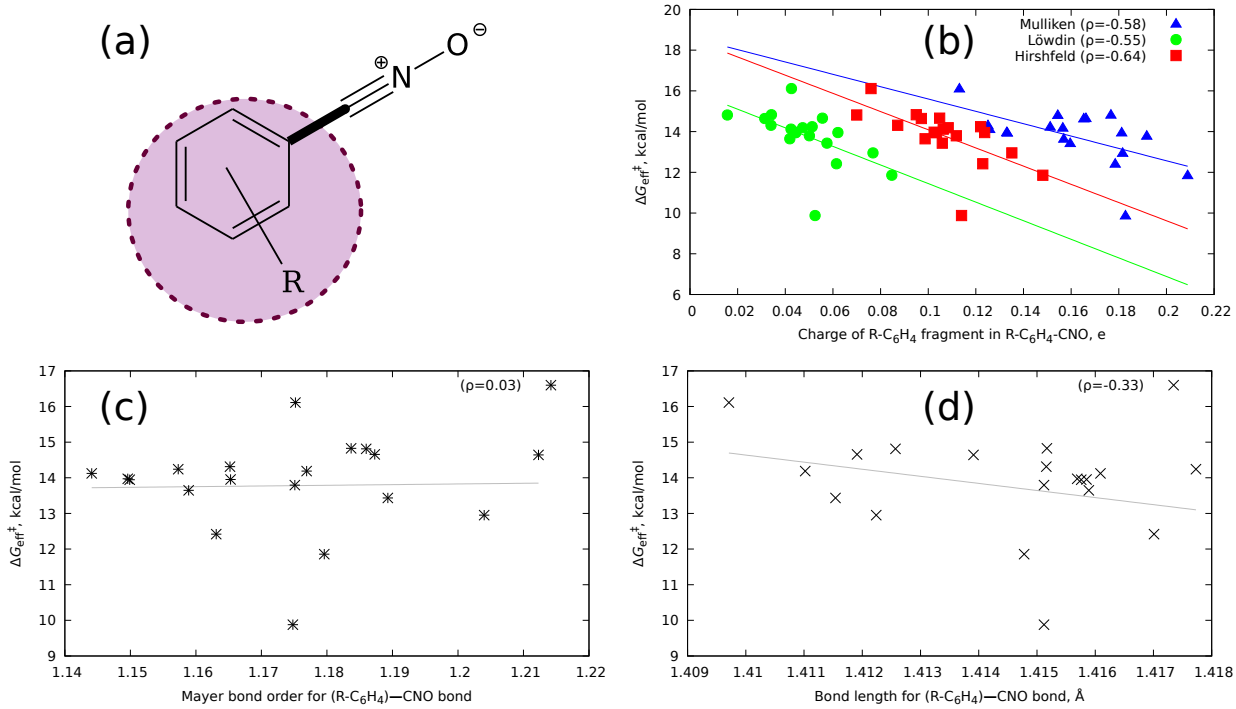

Figure 11: Correlation of the various descriptors, characterizing coupling between the substituted phenyl ring ($R-C_6H_4$) and the $-CNO$ group in the substituted PhCNO, demonstrated in Figure 10. (a) Shows the substituted reagent molecule with a violet circle denoting the two groups of atoms (within and outside the circle) used for charge calculations and the bold C-N bond indicating the bond for which Mayer bond orders and lengths were computed. (b) Correlation of net atomic charges of $R-C_6H_4$ fragment with the effective reaction barrier heights. (C) Correlation of the Mayer bond order of the C-N bond with the effective reaction barrier heights. (d) Correlation of the C-N bond length with the effective reaction barrier heights. All the calculations were done at the r^{2}SCAN-3c level of theory in benzene.

PCC being –0.85.

3 Conclusions

We have thoroughly investigated the mechanism of the Thiemann-type SO_2-mediated conversion of the phenylnitrile oxide (PhCNO) into phenyl isocyanate (PhNCO). The reaction proceeds through the five-membered ring intermediate, with reagents and products being separated from this intermediate by only a single transition state (Figures 3 and 5), respectively. Thus, we confirmed a previously proposed mechanism for this and similar reactions. In addition, we have suggested better inorganic catalysts for such rearrangement, namely SO_3 and SeO_2.

A small survey of the organic catalysts did not reveal any possible better candidates. However, as a byproduct, we found a mechanism of the reaction of PhCNO with the N-sulfinylaniline PhNSO that produces diphenyl carbodiimide ($Ph-N=C=N-Ph$). As it turns out, the reaction proceeds by a similar mechanism, through the formation of the five-membered ring and then eliminating SO_2 upon PhNCNPh formation. The PhNSO-catalyzed conversion PhCNO $\longrightarrow$ PhNCO is also a possible but less favorable reaction pathway, and it explains the found traces of PhNCO in the reaction mixture.[47, 48]

In the end, we also surveyed the effect of phenyl ring substituents on the reaction kinetics. It turns out that such substitution slows down the reaction with respect to the unsubstituted PhCNO. The reaction seems to proceed slower with the increasing electron-withdrawing effect of the substituent.

We also wanted to highlight that we tried to follow the unbiased data representation during this research to avoid the positive result bias.[49, 50] Namely, we reported both successful cases that we found and the dead-ends that we encountered, such as the N_2O, O_3 catalysis (Figure 7) or the highly improbable reactions of PhCNO with SO_2 (Figure 3).

This study was a popular social network-based, self-organized collaboration that yielded fruitful ideas generation and knowledge exchange. Therefore, we believe that we provide a proof-of-concept case for the possibilities of such web-based theoretical chemistry collaborations.

Methods

We used recommendations given in the publication by Bursch *et al.* as the starting point for our computations.[51] Quantum-chemical calculations were done using the ORCA 5,[52, 53] AMS 2021,[54] Firefly 8.2.0,[55] and Priroda[56] program suits. For drawing the 3D-molecular structures and for visualization of the calculation results, the Jmol,[25] ChemCraft,[57] and Molden[58, 59] molecular viewers were used.

The following quantum-chemical approximations were applied in the calculations. The DFT functionals applied were B3LYP,[60–62] PBE,[63] PBE0,[64] r^{2}SCAN,[65] ωB97X.[66] Dispersion corrections used were D3(BJ)[67] and D4.[68, 69] Along with DFT, optimizations of the structures and search for TS were done with the MP2 method.[70] Solvation effects were accounted for using conductor-like polarizable continuum model (CPCM),[71, 72] Conductor-like Screening Model (COSMO),[73–75] and a recently developed Solv model,[30] applied in SPT-V scheme. Based on the DFT geometries, the accurate single-point energies of the structures were obtained using the DLPNO-CCSD(T) level of theory,[76] including the CPCM-based results.[77] The basis sets used were 6-31G,[78] def2-TZVP, def2-TZVPP,[79] (aug)-cc-pVTZ, and cc-pVQZ.[80, 81] With DLPNO-CCSD(T) calculations, a complete basis set (CBS) extrapolation scheme CBS(3/4) based on cc-pVTZ and cc-pVQZ basis sets was applied.[82–84] The zeroth-order regular approximation (ZORA)[85] was used in reference DLPNO-CCSD(T1) calculations[86] together with CBS(3/4) extrapolation based on ZORA-def2-TZVPP and ZORA-def2-QZVPP basis sets[87] and 6/7 extrapolation to the complete PNO space.[26] In Priroda calculations, the Λ01 basis set was used[88, 89]. In AMS calculations, the TZ2P Slater-type-orbital basis set[90–92] was applied. A major part of DFT calculations was performed using the r^{2}SCAN-3c approximation.[93]

For the stable species (reagents, products, and intermediates), we performed geometry optimizations. Transition states (TS) between these species were identified using the nudged elastic band (NEB) method[94, 95] and scans along various internal coordinates. The local minimum and TS were confirmed by follow-up harmonic frequency calculations. To visualize the mechanism, intrinsic reaction coordinate (IRC) scans were performed.[96]

The bond-breaking Bohmian metadynamics (BBBMTD) simulations[97] of the isomerization in the intermediate were performed at the B3LYP-D3(BJ)/6-31G level of theory with PyRAMD[98, 99] software. ORCA 5 package was used as a source of the forces. The simulations were 5 ps in duration with 1 fs time step. The initial velocities were sampled from Maxwell-Boltzmann distribution at 300 K. The bias potential was updated every 10 fs with a Gaussian wavepacket width of σ = 0.05 Å. A Berendsen thermostat[100] at 300 K with a relaxation time of 100 fs was used to prevent overheating. Three sets of simulations with five trajectories were set. These sets differed by the collective variable (CV) definition.

More specific details about the calculations performed can be found in ESI.

Open data statement

The reaction energetic profiles and the optimized structures of the reagents, products, and transition states are provided in the ESI. As a part of ESI, we provide animations of the IRC scans. Raw data can be found in the GitLab repository: https://gitlab.com/madschumacher/crazyreactionstudy.

Author Contributions

SSL made the meme. DIS and DST proposed the idea of the project. SSL, MAK, AVB, RAO, DKK, VAM, VVD, and DIS have performed a literature survey. OBB, EAN, IG, SSL, MAK, EAI, AVB, OLD, AAC, IVP, RAZ, AAP, BOP, YVR, AMG and DST have performed theoretical calculations. OBB, EAN, IG, LEA, DST, and DIS analyzed the theoretical calculation results and made the figures. DST, MAK, LEA, IG, RAO, DKK, VVD, and DIS wrote the initial draft of the manuscript. OBB, EAN, IG, LEA, AMG, and DST made the ESI. All authors participated in discussions and evaluations of the manuscript.

Conflicts of interest

There are no conflicts to declare.

Acknowledgements

EAI's, OBB's, IVP's, and SSL's calculations have been carried out using computing resources of the federal collective usage center Complex for Simulation and Data Processing for Mega-science Facilities at NRC "Kurchatov Institute". AAC's calculations of reference reaction pathway were performed with the financial support of the Ministry of Science and Higher Education of the Russian Federation (Contract No. 075-03-2023-642). AAP's calculations have been carried out using computing resources of the Supercomputer "Sergey Korolev" at Supercomputing Center Samara University (http://hpc.ssau.ru/). BOP's and YVR's calculations were performed using the "Blokhin" HPC of the Center for collective use "Nanoscale Structure of Matter" of the Southern Federal University.

References

[1] V. I. Gorbatenko, E. Z. Zhuravlev, and L. I. Samarai. *Isocyanates. Synthesis and Properties of Alkyl-, Aryl-, and Heteroisocyanates. (in Russian)*. Naukova Dumka, Kiev, 1987.

[2] Shoichiro. Ozaki. Recent advances in isocyanate chemistry. *Chemical Reviews*, 72(5):457–496, 1972. doi: 10.1021/cr60279a002. URL https://doi.org/10.1021/cr60279a002.

[3] Joanna Niesiobedzka and Janusz Datta. Challenges and recent advances in bio-based isocyanate production. *Green Chem.*, 25:2482–2504, 2023. doi: 10.1039/D2GC04644J. URL http://dx.doi.org/10.1039/D2GC04644J.

[4] Reinhard Richter and Henri Ulrich. *Syntheses and preparative applications of isocyanates*, chapter 17, pages 619–818. John Wiley & Sons, Ltd, 1977. ISBN 9780470771532. doi: 10.1002/9780470771532.ch1. URL https://onlinelibrary.wiley.com/doi/abs/10.1002/9780470771532.ch1.

[5] Hans-Wilhelm Engels, Hans-Georg Pirkl, Reinhard Albers, Rolf W. Albach, Jens Krause, Andreas Hoffmann, Holger Casselmann, and Jeff Dormish. Polyurethanes: Versatile materials and sustainable problem solvers for today's challenges. *Angewandte Chemie International Edition*, 52(36):9422–9441, 2013. doi: 10.1002/anie.201302766. URL https://onlinelibrary.wiley.com/doi/abs/10.1002/anie.201302766.

[6] Berend Eling, Željko Tomović, and Volker Schädler. Current and future trends in polyurethanes: An industrial perspective. *Macromolecular Chemistry and Physics*, 221(14):2000114, 2020. doi: 10.1002/macp.202000114. URL https://onlinelibrary.wiley.com/doi/abs/10.1002/macp.202000114.

[7] Nina M.K. Lamba. *Polyurethanes in biomedical applications*. Taylor and Francis, 1998.

[8] Mark F. Sonnenschein. *Front Matter*. John Wiley & Sons, Ltd, 2021. ISBN 9781119669401. doi: 10.1002/9781119669401.fmatter. URL https://onlinelibrary.wiley.com/doi/abs/10.1002/9781119669401.fmatter.

[9] R.C. Gupta. Carbamate pesticides. In Philip Wexler, editor, *Encyclopedia of Toxicology (Third Edition)*, pages 661–664. Academic Press, Oxford, third edition edition, 2014. ISBN 978-0-12-386455-0. doi: 10.1016/B978-0-12-386454-3.00106-8. URL https://www.sciencedirect.com/science/article/pii/B9780123864543001068.

[10] Mikaël Thomas, Jérôme Alsarraf, Nahla Araji, Isabelle Tranoy-Opalinski, Brigitte Renoux, and Sébastien Papot. The lossen rearrangement from free hydroxamic acids. *Org. Biomol. Chem.*, 17:5420–5427, 2019. doi: 10.1039/C9OB00789J. URL http://dx.doi.org/10.1039/C9OB00789J.

[11] Pradip Debnath. Recent advances in the Hofmann rearrangement and its application to natural product synthesis. *Current Organic Chemistry*, 23(22):2402–2435, 2019. ISSN 1385-2728/1875-5348. doi: 10.2174/1385272823666191021115508.

[12] Isabelle Gillaizeau and Nicolas Gigant. *Alkyl and Acyl Azide Rearrangements*, chapter 4, pages 85–110. John Wiley & Sons, Ltd, 2015. ISBN 9781118939901. doi: 10.1002/9781118939901.ch4. URL https://onlinelibrary.wiley.com/doi/abs/10.1002/9781118939901.ch4.

[13] Arun K. Ghosh, Margherita Brindisi, and Anindya Sarkar. The Curtius rearrangement: Applications in modern drug discovery and medicinal chemistry. *ChemMedChem*, 13(22):2351–2373, 2018. doi: 10.1002/cmdc.201800518. URL https://chemistry-europe.onlinelibrary.wiley.com/doi/abs/10.1002/cmdc.201800518.

[14] Georg Trickes and Herbert Meier. Catalyzed rearrangement of nitrile oxides to isocyanates. *Angewandte Chemie International Edition in English*, 16(8):555–555, 1977. doi: 10.1002/anie.197705551. URL https://onlinelibrary.wiley.com/doi/abs/10.1002/anie.197705551.

[15] Initial post. https://vk.com/wall-196254731_3088, . Accessed: 2023-09-03.

[16] S. Gabriel and Max Koppe. Zur kenntniss des phenylnitromethans. *Berichte der deutschen chemischen Gesellschaft*, 19(1):1145–1148, 1886. doi: 10.1002/cber.188601901256. URL https://chemistry-europe.onlinelibrary.wiley.com/doi/abs/10.1002/cber.188601901256.

[17] Evgeny A. Pidko. Toward the balance between the reductionist and systems approaches in computational catalysis: Model versus method accuracy for the description of catalytic systems. *ACS Catalysis*, 7(7):4230–4234, 2017. doi: 10.1021/acscatal.7b00290. URL https://doi.org/10.1021/acscatal.7b00290.

[18] Yoshihiro Hayashi, Yuki Ishiyama, Toshikazu Takata, and Susumu Kawauchi. Exploration of unimolecular and bimolecular pathways for nitrile n-oxide isomerization to isocyanate through global reaction route mapping techniques. *European Journal of Organic Chemistry*, 2019(39):6646–6654, 2019. doi: 10.1002/ejoc.201901156. URL https://chemistry-europe.onlinelibrary.wiley.com/doi/abs/10.1002/ejoc.201901156.

[19] Florian J. Holsboer and Wolfgang Beck. Indo calculation of the fulminate–cyanate rearrangement. *J. Chem. Soc. D*, pages 262–263, 1970. doi: 10.1039/C29700000262. URL http://dx.doi.org/10.1039/C29700000262.

[20] Dieter Poppinger, Leo Radom, and John A. Pople. A theoretical study of the chno isomers. *Journal of the American Chemical Society*, 99(24):7806–7816, 1977. doi: 10.1021/ja00466a010. URL https://doi.org/10.1021/ja00466a010.

[21] W. K. Li, J. Baker, and L. Radom. Rearrangement of the fulminate anion (cno^-) to the cyanate anion (ocn^-). possible intermediacy of the oxazirinyl anion. *Australian Journal of Chemistry*, 39(6):913–921, 1986. doi: 10.1071/CH9860913. URL https://doi.org/10.1071/CH9860913.

[22] William R. Mitchell and R. Michael Paton. Flash vacuum pyrolysis of 1,2,5-oxadiazole 2-oxides and 1,2,3-triazole 1-oxides. *ARKIVOC*, 2010(10):34–54, Jul 2010. doi: 10.3998/ark.5550190.0011.a04. URL https://doi.org/10.3998/ark.5550190.0011.a04.

[23] Emmett H. Burk and Donald D. Carlos. Synthesis of organic isocyanates. i. thermal decomposition of substituted 1,3,2,4-dioxathiazole s-oxides. *Journal of Heterocyclic Chemistry*, 7(1):177–179, 1970. doi: 10.1002/jhet.5570070126. URL https://onlinelibrary.wiley.com/doi/abs/10.1002/jhet.5570070126.

[24] Initial post suggesting project. https://vk.com/@quant_chem_and_stuff-kvantovo-himicheskaya-stateinaya-piram . Accessed: 2023-09-03.

[25] Jmol: an open-source java viewer for chemical structures in 3d. URL http://www.jmol.org/.

[26] Ahmet Altun, Frank Neese, and Giovanni Bistoni. Extrapolation to the limit of a complete pair natural orbital space in local coupled-cluster calculations. *Journal of Chemical Theory and Computation*, 16(10):6142–6149, 2020. doi: 10.1021/acs.jctc.0c00344. URL https://doi.org/10.1021/acs.jctc.0c00344. PMID: 32897712.

[27] Chong Wha Pyun. Steady-state and equilibrium approximations in chemical kinetics. *Journal of Chemical Education*, 48(3):194, 1971. doi: 10.1021/ed048p194. URL https://doi.org/10.1021/ed048p194.

[28] Henry Eyring. The Activated Complex in Chemical Reactions. *The Journal of Chemical Physics*, 3(2):107–115, 11 2004. ISSN 0021-9606. doi: 10.1063/1.1749604. URL https://doi.org/10.1063/1.1749604.

[29] Keith J. Laidler and M. Christine King. Development of transition-state theory. *The Journal of Physical Chemistry*, 87(15):2657–2664, 1983. doi: 10.1021/j100238a002. URL https://doi.org/10.1021/j100238a002.

[30] Yury Minenkov. Solv: An alternative continuum model implementation based on fixed atomic charges, scaled particle theory, and the atom–atom potential method. *Journal of Chemical Theory and Computation*, 0(0):null, 0. doi: 10.1021/acs.jctc.3c00410. URL https://doi.org/10.1021/acs.jctc.3c00410. PMID: 37390470.

[31] Karl Dimroth, Christian Reichardt, Theodor Siepmann, and Ferdinand Bohlmann. Über pyridinium-n-phenol-betaine und ihre verwendung zur charakterisierung der polarität von lösungsmitteln. *Justus Liebigs Annalen der Chemie*, 661(1):1–37, 1963. doi: https://doi.org/10.1002/jlac.19636610102. URL https://chemistry-europe.onlinelibrary.wiley.com/doi/abs/10.1002/jlac.19636610102.

[32] Franco Cataldo. Application of reichardt's solvent polarity scale (et(30)) in the selection of bonding agents for composite solid rocket propellants. *Liquids*, 2(4):289–302, 2022. ISSN 2673-8015. doi: 10.3390/liquids2040017. URL https://www.mdpi.com/2673-8015/2/4/17.

[33] William E. Acree and Andrew S. I. D. Lang. Reichardt's dye-based solvent polarity and abraham solvent parameters: Examining correlations and predictive modeling. *Liquids*, 3(3):303–313, 2023. ISSN 2673-8015. doi: 10.3390/liquids3030020. URL https://www.mdpi.com/2673-8015/3/3/20.

[34] José P. Cerón-Carrasco, Denis Jacquemin, Christian Laurence, Aurélien Planchat, Christian Reichardt, and Khadija Sraïdi. Solvent polarity scales: determination of new et(30) values for 84 organic solvents. *Journal of Physical Organic Chemistry*, 27(6):512–518, 2014. doi: https://doi.org/10.1002/poc.3293. URL https://onlinelibrary.wiley.com/doi/abs/10.1002/poc.3293.

[35] Stefan Spange, Nadine Weiß, Caroline H. Schmidt, and Katja Schreiter. Reappraisal of empirical solvent polarity scales for organic solvents. *Chemistry–Methods*, 1(1):42–60, 2021. doi: https://doi.org/10.1002/cmtd.202000039. URL https://chemistry-europe.onlinelibrary.wiley.com/doi/abs/10.1002/cmtd.202000039.

[36] Biswanath Dinda. *General Aspects of Pericyclic Reactions*, pages 3–11. Springer International Publishing, Cham, 2017. ISBN 978-3-319-45934-9. doi: 10.1007/978-3-319-45934-9_1. URL https://doi.org/10.1007/978-3-319-45934-9_1.

[37] Yu Lan, Steven E. Wheeler, and K. N. Houk. Extraordinary difference in reactivity of ozone (ooo) and sulfur dioxide (oso): A theoretical study. *Journal of Chemical Theory and Computation*, 7(7):2104–2111, 2011. doi: 10.1021/ct200293w. URL https://doi.org/10.1021/ct200293w. PMID: 26606482.

[38] Beth A. Lindquist, Tyler Y. Takeshita, and Thom H. Jr. Dunning. Insights into the electronic structure of ozone and sulfur dioxide from generalized valence bond theory: Addition of hydrogen atoms. *The Journal of Physical Chemistry A*, 120(17):2720–2726, 2016. doi: 10.1021/acs.jpca.6b02014. URL https://doi.org/10.1021/acs.jpca.6b02014. PMID: 27070292.

[39] Harutoshi Takeo, Eizi Hirota, and Yonezo Morino. Third-order potential constants and dipole moment of seo2 by microwave spectroscopy. *Journal of Molecular Spectroscopy*, 41(2):420–422, 1972. ISSN 0022-2852. doi: https://doi.org/10.1016/0022-2852(72)90216-0. URL https://www.sciencedirect.com/science/article/pii/0022285272902160.

[40] Jacek Młochowski and Halina Wójtowicz-Młochowska. Developments in synthetic application of selenium(iv) oxide and organoselenium compounds as oxygen donors and oxygen-transfer agents. *Molecules*, 20(6):10205–10243, 2015. ISSN 1420-3049. doi: 10.3390/molecules200610205. URL https://www.mdpi.com/1420-3049/20/6/10205.

[41] Christin Gebhardt, Beate Priewisch, Elisabeth Irran, and Karola Rück-Braun. Oxidation of anilines with hydrogen peroxide and selenium dioxide as catalyst. *Synthesis*, 2008(12):1889–1894, Jun 2008. ISSN 0039-7881. doi: 10.1055/s-2008-1067088. URL http://www.thieme-connect.com/products/ejournals/abstract/10.1055/s-2008-1067088.

[42] Stefano Santoro, Juliano B. Azeredo, Vanessa Nascimento, Luca Sancineto, Antonio L. Braga, and Claudio Santi. The green side of the moon: ecofriendly aspects of organoselenium chemistry. *RSC Adv.*, 4:31521–31535, 2014. doi: 10.1039/C4RA04493B. URL http://dx.doi.org/10.1039/C4RA04493B.

[43] I. V. Bodrikov, V. L. Krasnov, and N. K. Tulegenova. Reaction of n-oxides of nitriles with sulfur trioxide. *Zh. Org. Khim.*, 14(10):2231, 1978.

[44] Vijay Nair, K.V. Radhakrishnan, Anilkumar G. Nair, and Mohan M. Bhadbhade. 1,3-dipolar cycloaddition of nitrile-n-oxides with 3,5-di-tert-butyl-1,2-benzoquinone: Facile formation of spiro-1,3-dioxazoles. *Tetrahedron Letters*, 37(31):5623–5626, 1996. ISSN 0040-4039. doi: https://doi.org/10.1016/0040-4039(96)01172-0. URL https://www.sciencedirect.com/science/article/pii/0040403996011720.

[45] Vijay Nair, K.V. Radhakrishnan, K.C. Sheela, and Nigam P. Rath. 1,3-dipolar cycloaddition reactions of nitrile-n-oxides with o-benzoquinones. *Tetrahedron*, 55(49):14199–14210, 1999. ISSN 0040-4020. doi: https://doi.org/10.1016/S0040-4020(99)00887-X. URL https://www.sciencedirect.com/science/article/pii/S004040209900887X.

[46] V.A. Soloshonok and V.P. Kukhar. *Zh. Org. Khim.*, 14(25):419, 1990.

[47] P. Rajagopalan and B. G. Advani. Dipolar addition reactions of nitrile oxides. ii.1 a new synthesis of carbodiimides. *The Journal of Organic Chemistry*, 30(10):3369–3371, 1965. doi: 10.1021/jo01021a025. URL https://doi.org/10.1021/jo01021a025.

[48] S. Rajagopalan, B. G. Advani, and C. N. Talaty. *Diphenylcarbodiimide, Method II*, pages 70–70. John Wiley & Sons, Ltd, 2003. ISBN 9780471264224. doi: 10.1002/0471264180.os049.19. URL https://onlinelibrary.wiley.com/doi/abs/10.1002/0471264180.os049.19.

[49] Susannah L. Scott, T. Brent Gunnoe, Paolo Fornasiero, and Cathleen M. Crudden. To err is human; to reproduce takes time. *ACS Catalysis*, 12(6):3644–3650, 2022. doi: 10.1021/acscatal.2c00967. URL https://doi.org/10.1021/acscatal.2c00967.

[50] A. Mlinarić, M. Horvat, and V. Šupak-Smolčić. Dealing with the positive publication bias: Why you should really publish your negative results. *Biochem Med*, 27(3):030201, 2017. doi: 10.11613/BM.2017.030201.

[51] Markus Bursch, Jan-Michael Mewes, Andreas Hansen, and Stefan Grimme. Best-practice dft protocols for basic molecular computational chemistry**. *Angewandte Chemie International Edition*, 61(42):e202205735, 2022. doi: 10.1002/anie.202205735. URL https://onlinelibrary.wiley.com/doi/abs/10.1002/anie.202205735.

[52] Frank Neese, Frank Wennmohs, Ute Becker, and Christoph Riplinger. The orca quantum chemistry program package. *The Journal of Chemical Physics*, 152(22):224108, 2020. doi: 10.1063/5.0004608. URL https://doi.org/10.1063/5.0004608.

[53] Frank Neese. Software update: The orca program system—version 5.0. *WIREs Computational Molecular Science*, 12(5):e1606, 2022. doi: 10.1002/wcms.1606. URL https://wires.onlinelibrary.wiley.com/doi/abs/10.1002/wcms.1606.

[54] G. te Velde, F. M. Bickelhaupt, E. J. Baerends, C. Fonseca Guerra, S. J. A. van Gisbergen, J. G. Snijders, and T. Ziegler. Chemistry with adf. *J. Comput. Chem.*, 22(9):931–967, 2001. ISSN 1096-987X. doi: 10.1002/jcc.1056. URL http://dx.doi.org/10.1002/jcc.1056.

[55] Alex A. Granovsky. Firefly version 8.2.0. URL http://classic.chem.msu.su/gran/firefly/index.html.

[56] D. N. Laikov and Yu. A. Ustynyuk. Priroda-04: a quantum-chemical program suite. new possibilities in the study of molecular systems with the application of parallel computing. *Russian Chemical Bulletin*, 54(3):820–826, Mar 2005. ISSN 1573-9171. doi: 10.1007/s11172-005-0329-x. URL https://doi.org/10.1007/s11172-005-0329-x.

[57] Chemcraft - graphical software for visualization of quantum chemistry computations. version 1.8, build 654. URL https://www.chemcraftprog.com.

[58] G. Schaftenaar and J. H. Noordik. Molden: a pre- and post-processing program for molecular and electronic structures*. *Journal of Computer-Aided Molecular Design*, 14(2):123–134, Feb 2000. ISSN 1573-4951. doi: 10.1023/A:1008193805436. URL https://doi.org/10.1023/A:1008193805436.

[59] Gijs Schaftenaar, Elias Vlieg, and Gert Vriend. Molden 2.0: quantum chemistry meets proteins. *Journal of Computer-Aided Molecular Design*, 31(9):789–800, Sep 2017. ISSN 1573-4951. doi: 10.1007/s10822-017-0042-5. URL https://doi.org/10.1007/s10822-017-0042-5.

[60] Axel D. Becke. Density-functional thermochemistry. iii. the role of exact exchange. *The Journal of Chemical Physics*, 98(7):5648–5652, 1993. doi: 10.1063/1.464913. URL http://link.aip.org/link/?JCP/98/5648/1.

[61] Chengteh Lee, Weitao Yang, and Robert G. Parr. Development of the colle-salvetti correlation-energy formula into a functional of the electron density. *Phys. Rev. B*, 37:785–789, Jan 1988. doi: 10.1103/physrevb.37.785. URL http://link.aps.org/doi/10.1103/PhysRevB.37.785.

[62] S. H. Vosko, L. Wilk, and M. Nusair. Accurate spin-dependent electron liquid correlation energies for local spin density calculations: a critical analysis. *Canadian Journal of Physics*, 58(8):1200–1211, 1980. doi: 10.1139/p80-159.

[63] John P. Perdew, Kieron Burke, and Matthias Ernzerhof. Generalized gradient approximation made simple [phys. rev. lett. 77, 3865 (1996)]. *Phys. Rev. Lett.*, 78:1396–1396, Feb 1997. doi: 10.1103/PhysRevLett.78.1396. URL https://link.aps.org/doi/10.1103/PhysRevLett.78.1396.

[64] Carlo Adamo and Vincenzo Barone. Toward reliable density functional methods without adjustable parameters: The pbe0 model. *The Journal of Chemical Physics*, 110(13):6158–6170, 1999. doi: 10.1063/1.478522. URL http://scitation.aip.org/content/aip/journal/jcp/110/13/10.1063/1.478522.

[65] James W. Furness, Aaron D. Kaplan, Jinliang Ning, John P. Perdew, and Jianwei Sun. Accurate and numerically efficient r2scan meta-generalized gradient approximation. *The Journal of Physical Chemistry Letters*, 11(19):8208–8215, 2020. doi: 10.1021/acs.jpclett.0c02405. URL https://doi.org/10.1021/acs.jpclett.0c02405. PMID: 32876454.

[66] Jeng-Da Chai and Martin Head-Gordon. Systematic optimization of long-range corrected hybrid density functionals. *The Journal of Chemical Physics*, 128(8):084106, 02 2008. ISSN 0021-9606. doi: 10.1063/1.2834918. URL https://doi.org/10.1063/1.2834918.

[67] Stefan Grimme, Stephan Ehrlich, and Lars Goerigk. Effect of the damping function in dispersion corrected density functional theory. *Journal of Computational Chemistry*, 32(7):1456–1465, 2011. doi: 10.1002/jcc.21759. URL https://onlinelibrary.wiley.com/doi/abs/10.1002/jcc.21759.

[68] Eike Caldeweyher, Sebastian Ehlert, Andreas Hansen, Hagen Neugebauer, Sebastian Spicher, Christoph Bannwarth, and Stefan Grimme. A generally applicable atomic-charge dependent London dispersion correction. *The Journal of Chemical Physics*, 150(15):154122, 04 2019. ISSN 0021-9606. doi: 10.1063/1.5090222. URL https://doi.org/10.1063/1.5090222.

[69] Eike Caldeweyher, Jan-Michael Mewes, Sebastian Ehlert, and Stefan Grimme. Extension and evaluation of the d4 london-dispersion model for periodic systems. *Phys. Chem. Chem. Phys.*, 22:8499–8512, 2020. doi: 10.1039/D0CP00502A. URL http://dx.doi.org/10.1039/D0CP00502A.

[70] Chr. Møller and M. S. Plesset. Note on an approximation treatment for many-electron systems. *Physical Review*, 46(7):618–622, Oct 1934. doi: 10.1103/physrev.46.618.

[71] Darrin M. York and Martin Karplus. A smooth solvation potential based on the conductor-like screening model. *The Journal of Physical Chemistry A*, 103(50):11060–11079, 1999. doi: 10.1021/jp9920971. URL https://doi.org/10.1021/jp9920971.

[72] Aleksandr V. Marenich, Christopher J. Cramer, and Donald G. Truhlar. Universal solvation model based on solute electron density and on a continuum model of the solvent defined by the bulk dielectric constant and atomic surface tensions. *The Journal of Physical Chemistry B*, 113(18):6378–6396, 2009. doi: 10.1021/jp810292n. URL https://doi.org/10.1021/jp810292n. PMID: 19366259.

[73] A. Klamt and G. Schüürmann. Cosmo: a new approach to dielectric screening in solvents with explicit expressions for the screening energy and its gradient. *J. Chem. Soc., Perkin Trans. 2*, pages 799–805, 1993. doi: 10.1039/P29930000799. URL http://dx.doi.org/10.1039/P29930000799.

[74] Andreas Klamt. Conductor-like screening model for real solvents: A new approach to the quantitative calculation of solvation phenomena. *The Journal of Physical Chemistry*, 99(7):2224–2235, 1995. doi: 10.1021/j100007a062. URL https://doi.org/10.1021/j100007a062.

[75] Andreas Klamt and Volker Jonas. Treatment of the outlying charge in continuum solvation models. *The Journal of Chemical Physics*, 105(22):9972–9981, 12 1996. ISSN 0021-9606. doi: 10.1063/1.472829. URL https://doi.org/10.1063/1.472829.

[76] Christoph Riplinger and Frank Neese. An efficient and near linear scaling pair natural orbital based local coupled cluster method. *The Journal of Chemical Physics*, 138(3):034106, 01 2013. ISSN 0021-9606. doi: 10.1063/1.4773581. URL https://doi.org/10.1063/1.4773581.

[77] Miquel Garcia-Ratés, Ute Becker, and Frank Neese. Implicit solvation in domain based pair natural orbital coupled cluster (dlpno-ccsd) theory. *Journal of Computational Chemistry*, 42(27):1959–1973, 2021. doi: 10.1002/jcc.26726. URL https://onlinelibrary.wiley.com/doi/abs/10.1002/jcc.26726.

[78] W. J. Hehre, R. Ditchfield, and J. A. Pople. Self—consistent molecular orbital methods. xii. further extensions of gaussian—type basis sets for use in molecular orbital studies of organic molecules. *The Journal of Chemical Physics*, 56(5):2257–2261, 1972. doi: 10.1063/1.1677527. URL https://doi.org/10.1063/1.1677527.

[79] Florian Weigend and Reinhart Ahlrichs. Balanced basis sets of split valence, triple zeta valence and quadruple zeta valence quality for h to rn: Design and assessment of accuracy. *Phys. Chem. Chem. Phys.*, 7:3297–3305, 2005. doi: 10.1039/B508541A. URL http://dx.doi.org/10.1039/B508541A.

[80] Thom H. Dunning. Gaussian basis sets for use in correlated molecular calculations. i. the atoms boron through neon and hydrogen. *The Journal of Chemical Physics*, 90(2):1007–1023, 1989. doi: 10.1063/1.456153. URL https://doi.org/10.1063/1.456153.

[81] Rick A. Kendall, Thom H. Dunning, and Robert J. Harrison. Electron affinities of the first-row atoms revisited. systematic basis sets and wave functions. *The Journal of Chemical Physics*, 96(9):6796–6806, 1992. doi: 10.1063/1.462569. URL https://doi.org/10.1063/1.462569.

[82] Shijun Zhong, Ericka C. Barnes, and George A. Petersson. Uniformly convergent n-tuple-ζ augmented polarized (nzap) basis sets for complete basis set extrapolations. i. self-consistent field energies. *The Journal of Chemical Physics*, 129(18):184116, 2008. doi: 10.1063/1.3009651. URL https://doi.org/10.1063/1.3009651.

[83] Frank Neese and Edward F. Valeev. Revisiting the atomic natural orbital approach for basis sets: Robust systematic basis sets for explicitly correlated and conventional correlated ab initio methods? *Journal of Chemical Theory and Computation*, 7(1):33–43, 2011. doi: 10.1021/ct100396y. URL https://doi.org/10.1021/ct100396y. PMID: 26606216.

[84] Trygve Helgaker, Wim Klopper, Henrik Koch, and Jozef Noga. Basis-set convergence of correlated calculations on water. *The Journal of Chemical Physics*, 106(23):9639–9646, 1997. doi: 10.1063/1.473863. URL https://doi.org/10.1063/1.473863.

[85] E. van Lenthe, E. J. Baerends, and J. G. Snijders. Relativistic regular two-component Hamiltonians. *The Journal of Chemical Physics*, 99(6):4597–4610, 09 1993. ISSN 0021-9606. doi: 10.1063/1.466059. URL https://doi.org/10.1063/1.466059.

[86] Yang Guo, Christoph Riplinger, Ute Becker, Dimitrios G. Liakos, Yury Minenkov, Luigi Cavallo, and Frank Neese. Communication: An improved linear scaling perturbative triples correction for the domain based local pair-natural orbital based singles and doubles coupled cluster method [DLPNO-CCSD(T)]. *The Journal of Chemical Physics*, 148(1):011101, 01 2018. ISSN 0021-9606. doi: 10.1063/1.5011798. URL https://doi.org/10.1063/1.5011798.

[87] Florian Weigend and Reinhart Ahlrichs. Balanced basis sets of split valence, triple zeta valence and quadruple zeta valence quality for h to rn: Design and assessment of accuracy. *Phys. Chem. Chem. Phys.*, 7:3297–3305, 2005. doi: 10.1039/B508541A. URL http://dx.doi.org/10.1039/B508541A.

[88] Dimitri N. Laikov. A new class of atomic basis functions for accurate electronic structure calculations of molecules. *Chemical Physics Letters*, 416(1):116–120, 2005. ISSN 0009-2614. doi: 10.1016/j.cplett.2005.09.046. URL https://www.sciencedirect.com/science/article/pii/S0009261405014120.

[89] Dimitri N. Laikov. Atomic basis functions for molecular electronic structure calculations. *Theoretical Chemistry Accounts*, 138(3):40, Mar 2019. ISSN 1432-2234. doi: 10.1007/s00214-019-2432-3. URL https://doi.org/10.1007/s00214-019-2432-3.

[90] E. Van Lenthe and E. J. Baerends. Optimized slater-type basis sets for the elements 1–118. *Journal of Computational Chemistry*, 24(9):1142–1156, 2003. doi: 10.1002/jcc.10255. URL https://onlinelibrary.wiley.com/doi/abs/10.1002/jcc.10255.

[91] Delano P. Chong, Erik Van Lenthe, Stan Van Gisbergen, and Evert Jan Baerends. Even-tempered slater-type orbitals revisited: From hydrogen to krypton. *Journal of Computational Chemistry*, 25(8):1030–1036, 2004. doi: 10.1002/jcc.20030. URL https://onlinelibrary.wiley.com/doi/abs/10.1002/jcc.20030.

[92] D.P. Chong. Augmenting basis set for time-dependent density functional theory calculation of excitation energies: Slater-type orbitals for hydrogen to krypton. *Molecular Physics*, 103(6-8):749–761, 2005. doi: 10.1080/00268970412331333618. URL https://doi.org/10.1080/00268970412331333618.

[93] Stefan Grimme, Andreas Hansen, Sebastian Ehlert, and Jan-Michael Mewes. r2SCAN-3c: A "Swiss army knife" composite electronic-structure method. *The Journal of Chemical Physics*, 154(6):064103, 02 2021. ISSN 0021-9606. doi: 10.1063/5.0040021. URL https://doi.org/10.1063/5.0040021.

[94] Gregory Mills, Hannes Jónsson, and Gregory K. Schenter. Reversible work transition state theory: application to dissociative adsorption of hydrogen. *Surface Science*, 324(2):305–337, 1995. ISSN 0039-6028. doi: 10.1016/0039-6028(94)00731-4. URL https://www.sciencedirect.com/science/article/pii/0039602894007314.

[95] Vilhjálmur Ásgeirsson, Benedikt Orri Birgisson, Ragnar Bjornsson, Ute Becker, Frank Neese, Christoph Riplinger, and Hannes Jónsson. Nudged elastic band method for molecular reactions using energy-weighted springs combined with eigenvector following. *Journal of Chemical Theory and Computation*, 17(8):4929–4945, 2021. doi: 10.1021/acs.jctc.1c00462. URL https://doi.org/10.1021/acs.jctc.1c00462. PMID: 34275279.

[96] Kazuhiro Ishida, Keiji Morokuma, and Andrew Komornicki. The intrinsic reaction coordinate. an ab initio calculation for hnc→hcn and h-+ch4→ch4+h-. *The Journal of Chemical Physics*, 66(5):2153–2156, 08 2008. ISSN 0021-9606. doi: 10.1063/1.434152. URL https://doi.org/10.1063/1.434152.

[97] Denis S. Tikhonov. Metadynamics simulations with bohmian-style bias potential. *Journal of Computational Chemistry*, 44(21):1771–1775, 2023. doi: 10.1002/jcc.27125. URL https://onlinelibrary.wiley.com/doi/abs/10.1002/jcc.27125.

[98] Denis S. Tikhonov. Pyramd manual. https://confluence.desy.de/display/CFA/PyRAMD, 2021.

[99] Denis S. Tikhonov. Pyramd. https://stash.desy.de/projects/PYRAMD/repos/pyramd/browse, 2021.

[100] H. J. C. Berendsen, J. P. M. Postma, W. F. van Gunsteren, A. DiNola, and J. R. Haak. Molecular dynamics with coupling to an external bath. *The Journal of Chemical Physics*, 81(8):3684–3690, 10 1984. ISSN 0021-9606. doi: 10.1063/1.448118. URL https://doi.org/10.1063/1.448118.